

# Polymer Chemistry

Accepted Manuscript



This is an *Accepted Manuscript*, which has been through the Royal Society of Chemistry peer review process and has been accepted for publication.

*Accepted Manuscripts* are published online shortly after acceptance, before technical editing, formatting and proof reading. Using this free service, authors can make their results available to the community, in citable form, before we publish the edited article. We will replace this *Accepted Manuscript* with the edited and formatted *Advance Article* as soon as it is available.

You can find more information about *Accepted Manuscripts* in the [Information for Authors](#).

Please note that technical editing may introduce minor changes to the text and/or graphics, which may alter content. The journal's standard [Terms & Conditions](#) and the [Ethical guidelines](#) still apply. In no event shall the Royal Society of Chemistry be held responsible for any errors or omissions in this *Accepted Manuscript* or any consequences arising from the use of any information it contains.

## ARTICLE

## Effect of Ring Size on the Mechanical Relaxation Dynamics of Polyrotaxane Gels

Cite this: DOI: 10.1039/x0xx00000x

K. Kato,\* K. Karube, N. Nakamura and K. Ito\*,

Received 00th January 2012,  
Accepted 00th January 2012

DOI: 10.1039/x0xx00000x

[www.rsc.org/](http://www.rsc.org/)

Mechanically interlocked molecules have unique intramolecular dynamics owing to the relative motion of different components. Although the characteristic molecular dynamics in solution can be controlled by the design of their components, this generally does not define the macroscopic material properties. We demonstrate that the size of the ring components in polyrotaxanes significantly affect the mechanical relaxation dynamics of their cross-linked gels through the relative translational motion of polymer chains and cross-links. We synthesized a size-mismatched polyrotaxane consisting of polyethylene glycol (PEG) and  $\gamma$ -cyclodextrins ( $\gamma$ -CDs) for comparison with a size-matched polyrotaxane with smaller rings of  $\alpha$ -cyclodextrins ( $\alpha$ -CDs). Each polyrotaxane was cross-linked in solution to form gels whose networked polymer chains could slide through the cross-links formed by the CDs. Viscoelastic measurements of the gels showed similar stress relaxation behaviors, with relaxation times considerably longer for gels with larger rings. Detailed analyses of the relaxation dynamics revealed that the stress relaxation corresponded to the dynamics of chain sliding through the cross-links and that the difference in dynamics is attributable to the difference in friction in the ring cavity. The increased friction is explainable by enhanced interactions caused by penetration of solvent molecules in the extra cavity of  $\gamma$ -CD, as supported by NMR relaxation measurements and molecular modeling.

### Introduction

The molecular dynamics of polymeric materials strongly correlates with the mechanical properties. Depending on the characteristic times of the molecular dynamics, polymer materials behave as viscous fluids or elastic solids, a property called viscoelasticity. Local segmental motions, called micro-Brownian motion, relate to the glass transition,<sup>1</sup> and the diffusion of an entire chain defines the flow of a material.<sup>2</sup> A molecular interpretation of the molecular dynamics enables the creation of various molecular designs to control the mechanical properties. The segmental motion can be controlled e.g., by the interaction among chains, where the introduction of polar substituents generally results in an increased glass transition temperature.<sup>3</sup> The material flow can be precisely controlled e.g., by the chain length, where longer chains make the flow slower, and thus cross-linked polymer chains prevent flow.<sup>4</sup> These universal molecular designs are widely utilized to control the processing and mechanical properties of polymeric materials.

In addition to the dynamics of polymer chains, mechanically interlocked polymers, such as polyrotaxanes (PRs), have a relative motion between two different components: the sliding of rings along the polymer chain. The dynamics of the microscopic sliding in solution has been investigated by e.g., NMR and neutron spin echo spectroscopies.<sup>5-8</sup> More systematic

studies on the sliding dynamics have been performed using simpler molecules with shorter backbones, called molecular shuttles, indicating a significant influence of the chemical structure of the backbone on the dynamics.<sup>9-11</sup> A series of studies on the dynamics of inclusion crystals of cyclodextrins (CDs) with various guest polymer end groups has revealed that the bulkiness and charge of the end groups varied the complexation dynamics.<sup>12,13</sup> These results provide strategies for molecular design based on the interactions between different components to control the dynamics of sliding in PRs.

The microscopic sliding dynamics, however, do not affect the macroscopic properties, neither in solution nor in the solid state. On the other hand, polymer gels made from PRs, called polyrotaxane gels, were recently found to exhibit a peculiar mechanical relaxation owing to the sliding dynamics.<sup>14,15</sup> Since polyrotaxane gels are synthesized by cross-linking PRs via ring components, the polymer chains in the network can slide through the cross-links.<sup>16</sup> It is thought that chain sliding enables the relaxation of stress applied to the network, appearing as a viscoelastic relaxation. Therefore, it is expected that the mechanical properties of the gels can be controlled by the appropriate molecular design of the backbone and ring components.

Herein, we report the distinct macroscopic dynamics observed by viscoelastic measurements of two different polyrotaxane gels,  $\alpha$ -PR and  $\gamma$ -PR gels, which have different-sized ring

components,  $\alpha$ -CD and  $\gamma$ -CD, respectively, with a common backbone polymer, polyethylene glycol (PEG) (Fig. 1). First, we describe an efficient synthesis of  $\gamma$ -PR, which is a single-stranded PR of PEG and  $\gamma$ -CD. The obtained  $\gamma$ -PR is appropriate for comparison with  $\alpha$ -PR, because the only difference between these two systems is the size of the ring component. Then, we compare the viscoelastic relaxation dynamics of the polyrotaxane gels prepared from the PRs with different ring components. Detailed analyses of the dynamics revealed a common relaxation mechanism with significantly different frictional forces in the gels with different-sized rings.

**Fig. 1** Polyrotaxanes and their cross-linked gels (polyrotaxane gels) with different-sized cyclodextrins (CDs).

## Experimental Section

**Materials.** Bis(*p*-nitrophenyl ester)-terminated PEG (PEG-NP), in which 89% of the terminal groups are activated, was purchased from NOF Corporation; its number average molecular weight,  $M_n$ , and weight average molecular weight,  $M_w$ , values were 21,000 and 24,000, respectively, as determined by size exclusion chromatography (SEC) with a calibration curve obtained using PEG standards purchased from Polymer Source Inc. The  $\gamma$ -cyclodextrin ( $\gamma$ -CD) was purchased from Wacker Chemie AG (CD content > 98.0%). A crude polyrotaxane consisting of PEG ( $M_n = 20,000$ ) and  $\alpha$ -CD ( $\alpha$ -PR) was purchased from Advanced Softmaterials Inc. and purified before use. *N,N'*-Dicyclohexylcarbodiimide (DCC) was purchased from Aldrich. *N*-ethyl-diisopropylamine, hexamethylene diisocyanate, anhydrous solvents, and other chemicals were purchased from Wako Pure Chemical Industries, Ltd. All reagents were used without further purification, except for  $\alpha$ -PR.

**Synthesis and purification of polyrotaxanes and polyrotaxane gels.**  $\gamma$ -PR, consisting of PEG and  $\gamma$ -CD, was synthesized by the reaction scheme shown in Fig. 2. The detailed procedure is given in ESI†. Purchased crude  $\alpha$ -PR was purified by repeated precipitation in deionized water. The two polyrotaxanes,  $\alpha$ -PR and  $\gamma$ -PR, were dissolved in DMSO and then cross-linked by hexamethylene diisocyanate to obtain gels. In each series of gels, five gels with different cross-linker concentrations were prepared in a thickness-controlled mold (thickness: 3.0 mm). After quenching the reaction, the gels immersed in DMSO were allowed to reach their equilibrium swelling. The treated gels were cylindrical with a diameter of  $21 \pm 1$  mm and thickness of  $3.3 \pm 0.3$  mm. The obtained  $\alpha$ -PR and  $\gamma$ -PR gels were designated  $\alpha$ -PR-g1 to g5 and  $\gamma$ -PR-g1 to g5, respectively. More detailed preparation procedures for these gels are described in ESI†.

**Fig. 2** Synthetic scheme of  $\gamma$ -PR by end-capping via transesterification with unthreaded excess  $\gamma$ -CD.

**Measurements for polyrotaxanes.**  $^1\text{H}$  NMR spectra at 400 MHz were recorded at 343 K on a JEOL ECS-400 NMR spectrometer. Spin-lattice relaxation times of protons,  $T_1(^1\text{H})$ s, were determined by inversion-recovery pulse sequences. SEC with DMSO/LiBr as the eluent was performed on two Shodex OHpak SB-G columns at 323 K using refractive index (RI)

detection and PEG standards. The LiBr concentration was 10 mM.

**Viscoelastic measurements.** Dynamic viscoelastic measurements were conducted with a strain-controlled oscillatory rheometer (RSAIII, TA Instruments) using a parallel plate geometry. The bottom plate was attached to a Petri dish filled with DMSO. All measurements were conducted in solvent to prevent the gels from drying. A common initial compression with 0.2% strain was loaded in advance and then frequency sweeps were conducted from 0.06 to 500  $\text{rad s}^{-1}$  at 298 K, applying 0.1% of the compressive oscillatory strain amplitude, which was within the range of linear viscoelasticity. Viscoelastic data were fit by the following equation, which is essentially identical to the Havriliak-Negami equation, to estimate the plateau moduli at high and low frequency limits and the relaxation time:<sup>17</sup>

$$E_{(\omega)}^* = E_{\infty} - \frac{\Delta E}{(1 + (i\omega\tau_{\text{HN}})^{\alpha})^{\beta}} \quad (1)$$

where  $\omega$  is the angular frequency,  $\Delta E$  is the relaxation strength,  $E_{\infty}$  is the storage modulus  $E'$  at the high frequency limit,  $\alpha$  and  $\beta$  are the exponential parameters that describe the broadness and asymmetry of the spectra, respectively, and  $\tau_{\text{HN}}$  is the nominal relaxation time. From these parameters, the relaxation time  $\tau_s$  associated with the maximum of  $E''$  was obtained by the following equation:<sup>18</sup>

$$\tau_s = \tau_{\text{HN}} \left[ \frac{\sin\left(\frac{\pi\alpha\beta}{2(\beta+1)}\right)}{\sin\left(\frac{\pi\alpha}{2(\beta+1)}\right)} \right]^{\frac{1}{\alpha}} \quad (2)$$

**Molecular modeling.** Geometric optimization of the inclusion complexes of PEG and CDs in the presence of DMSO were carried out using the MM2 force field as implemented in ChemBio3D. Refined X-ray coordinates were used as starting geometries of  $\alpha$ -CD and  $\gamma$ -CD. The heptamer of ethylene glycol was employed as a model compound for PEG and several DMSO molecules were threaded and located in the cavities at the starting point.

## Results and Discussion

**Synthesis and characterization of polyrotaxanes.** The synthesis of  $\alpha$ -PR, a polyrotaxane composed of PEG and  $\alpha$ -CD, has been established<sup>19</sup> based on the efficient inclusion complexation provided by the size match between the cavity and PEG.<sup>20</sup> On the other hand, a size-mismatched  $\gamma$ -PR is not easily synthesized,<sup>21</sup> because  $\gamma$ -CD does not efficiently complex with PEG. In some special cases, the large host cavity can include double strands of PEG with MW < 3400,<sup>23-25</sup> likely due to the introduction of bulky groups to the guest polymers. Here, we synthesized a size-mismatched single-stranded  $\gamma$ -PR by the scheme shown in Fig. 2. We have previously reported that the synthetic scheme is applicable to various polyrotaxanes that consist of size-matched CDs and guests.<sup>26</sup> In this method, the PEG end groups are converted into *p*-nitrophenyl ester in advance, so that the subsequent end-capping via transesterification with unthreaded  $\gamma$ -CD can be conducted efficiently. In addition, this end group seemed to aid in the complexation between  $\gamma$ -CD and PEG. Unmodified PEG, which has hydroxyl end groups, and PEG with carboxyl end groups do not form inclusion complexes, which can usually be observed

as a white precipitate. However, nitrophenylated PEG (PEG-NP) yielded a white precipitate of the complex, indicating the formation of a complex with  $\gamma$ -CD.

The production of PR by end-capping the inclusion complex was confirmed by SEC in dilute conditions with a good solvent that readily induces the dissociation of other types of complexes. SEC chromatograms of  $\alpha$ -PR and  $\gamma$ -PR, with a PEG reference, are shown in Fig. 3a. Each PR exhibited a single peak of higher molecular weight than PEG, though negligible amounts of free CDs existed. Molecular weights of  $\alpha$ -PR and  $\gamma$ -PR, estimated from a calibration curve obtained using PEG standards, were  $M_n = 64,000$  ( $M_w = 95,000$ ) and  $M_n = 87,000$  ( $M_w = 120,000$ ), respectively. A slight increase in the dispersity of the PEG component ( $M_w / M_n = 1.14$ ) indicates that the PRs have some variation in the number of CDs threaded. In addition, the refractive indices of the products became much higher than that of PEG, indicating that the products consist of components that have relatively high refractive indices, which are CDs as confirmed by  $^1\text{H}$  NMR spectra as mentioned below.

The composition of the products and ratios of components were analyzed by  $^1\text{H}$  NMR, with spectra of  $\gamma$ -PR and  $\alpha$ -PR shown in Fig. 3b. All PR signals were assigned to the protons of either CD or PEG and show good stoichiometric agreement within each component. The detailed assignments of CD protons were supported by  $^1\text{H}$ - $^1\text{H}$  COSY NMR spectra (see Figs S1 and S2 in ESI†). The integral values of each component show that the molar ratio of the CDs and PEG repeat unit is the same for both PRs, indicating the number of threaded CDs per PEG chain is the same. The average number of CDs per PEG chain is ca. 65.

**Fig. 3** (a) SEC traces (eluent: DMSO with 10 mM LiBr, sample concentration: 2 mg mL<sup>-1</sup>, detection: RI) and (b)  $^1\text{H}$  NMR spectra (400 MHz, DMSO-*d*<sub>6</sub>, 343K) of polyrotaxanes with different-sized rings:  $\alpha$ -PR and  $\gamma$ -PR.

In  $\gamma$ -PR, the large rings do not necessarily include a single strand of PEG, and instead may capture two chains in the cavity. Fig. 4 shows three possible structures of  $\gamma$ -PR: single-stranded, double-stranded, and partially double-stranded. Note that the molar ratio between PEG and  $\gamma$ -CD is constant, because the ratio was determined by  $^1\text{H}$  NMR unambiguously. When we assume  $\gamma$ -PR is single-stranded (Fig. 4a), the increase in molecular weight compared with  $\alpha$ -PR (ca. 1.3 times) comes only from the increased molecular weight of the ring component. The coverage, which is a measure of the CD packing density along the polymer backbone, is the same as that of  $\alpha$ -PR and is calculated to be 28%. On the other hand, a double-stranded polyrotaxane (Fig. 4b) should have twice the molecular weight of a single-stranded one. Thus, the molecular weight of  $\gamma$ -PR should be more than double for  $\alpha$ -PR. Additionally, the coverage should be exactly twice that of  $\alpha$ -PR. In actuality, the measured molecular weight of  $\gamma$ -PR was much less than double of that of  $\alpha$ -PR; the molecular weight increased by almost 1.3 times.

**Fig. 4** Three possible structures of  $\gamma$ -PR. Note that the molar ratio between PEG and  $\gamma$ -CD is the same for each.

In addition, when we consider that the respective  $\gamma$ -CDs in the same polyrotaxane do not necessarily include two identical strands (Fig. 4c), the significant increase in molecular weight is

unavoidable. However, such expected behavior was not observed by SEC, and the dispersity of  $\gamma$ -PR is the same as that of  $\alpha$ -PR. Therefore, it is reasonable to conclude that  $\gamma$ -PR is a single-stranded polyrotaxane similar to  $\alpha$ -PR, and thus the coverage of both PRs is the same. Characteristics of these two PRs and the yield of  $\gamma$ -PR are summarized in Table 1. The only difference in structure between these two PRs is the size of the ring component. The coverage is known to depend on the molecular weight of PEG; PR with high coverage (75~100%) is obtained from PEG with  $MW < 2000$ , the coverage decreases with the increase of the molecular weight, and it becomes almost constant (20~25%) with  $MW > 30000$ .<sup>27-29</sup> A theoretical calculation with a lattice model reproduced those experimentally obtained dependence, indicating that the coverage is determined by the balance between enthalpic gain due to the hydrophobic interaction and hydrogen bonds between adjacent CDs and loss due to the limited conformational entropy by the inclusion.<sup>30</sup> The fact that the polydispersity of PRs only slightly larger suggests such stable coverages at certain  $MW$  of PEG. And, we know experimentally that the constant coverage reproduces as long as we start from PEG with similar  $MW$  under similar inclusion condition, though significantly high temperature increases the entropic loss to yield PRs with very low coverages.<sup>31</sup> Thus, the identical coverages of the two PRs is not a coincidence, but probably indicates a common mechanism for the complexation between PEG and CDs of different sizes.

**Table 1.** Summary of polyrotaxanes.

	$M_n$	$M_w/M_n$	coverage <sup>*1</sup>	$w_{\text{PEG}}$ <sup>*2</sup>	yield <sup>*3</sup>
$\alpha$ -PR	64000	1.48	28%	0.24	—
$\gamma$ -PR	87000	1.38	28%	0.20	32%

<sup>\*1</sup> Calculated from the molar ratio of the CDs and repeating PEG unit based on a definition described in ESI†. <sup>\*2</sup> Weight fraction of PEG in the polyrotaxane. <sup>\*3</sup> Yields based on polymers.

**Viscoelastic properties of polyrotaxane gels.** Both precursor polyrotaxanes,  $\gamma$ -PR and  $\alpha$ -PR, were cross-linked in DMSO to yield polyrotaxane gels. Five gels were prepared from each polyrotaxane with different concentrations of cross-linker. Incidentally, the employed cross-linker concentrations exceed the equivalent amount of the ring components (1.1–2.9 times for  $\alpha$ -PR, 2.0–3.4 times for  $\gamma$ -PR), because less cross-linkers could not form infinite network; such cross-linking reactions generally require exceed amounts of cross-linkers because of the deceleration of diffusion of polymers and the formation of inhomogeneous network with the development of the reactions. Frequency dependences of the dynamic storage Young's modulus  $E'$  and the loss modulus  $E''$  of  $\gamma$ -PR and  $\alpha$ -PR gels are shown in Figs 5 and 6, respectively. Each series of gels exhibited significant relaxations, showing two plateaus for  $E'$  at both high and low frequency limits. These viscoelastic data were accurately fit by a semi-empirical equation, Eq. 1, indicated by the solid curves in the Figs.; the fit parameters and relaxation times  $\tau_s$  are summarized in Table S1 (in ESI†). In each series of gels,  $\tau_s$  decreases with an increase in cross-linker concentration, as can also be seen from the peak shift of  $E''$  to a higher frequency. The increase of cross-linker concentration simultaneously induced an increase in the higher plateau modulus,  $E_{\infty}$ . This indicates that the macroscopic relaxation time is correlated with the cross-linking density.

The average molecular weight between cross-links,  $M_x$ , which is inversely proportional to the cross-linking density, can be estimated from the Young's modulus,  $E_r$ , based on classical rubber theory by considering the solvent swelling of as-prepared gels:<sup>32</sup>

$$M_x = \frac{3\rho RT}{E_r} \phi^{-\frac{2}{3}}, \quad (3)$$

where  $R$  is the gas constant,  $T$  is the absolute temperature, and  $\phi$  is the ratio of volumes of the as-prepared and equilibrated gels ( $V_0/V$ ). The parameter  $\rho$  is the concentration of the network that

**Fig. 5** Storage and loss Young's moduli  $E'$  and  $E''$  of  $\alpha$ -PR gels at 298 K with different cross-linker concentrations (0.75, 1.00, 1.25, 1.50 and 2.00 vol% from g1 to g5). The solid curves were fit using Eq. 1.

**Fig. 6** Storage and loss Young's moduli  $E'$  and  $E''$  of  $\gamma$ -PR gels at 298 K with different cross-linker concentrations (1.50, 1.75, 2.00, 2.25 and 2.50 vol% from g1 to g5). The solid curves were fit using Eq. 1.

**Table 2.** Characteristics of  $\alpha$ - and  $\gamma$ -PR gels.

	$\rho$ [ $10^3$ g/m <sup>3</sup> ] <sup>*1</sup>	$\phi$	$M_x$ [g/mol]	$n_{CD}$	
$\alpha$ -PR	-g1	0.91	0.838	7380	5.7
	-g2	1.12	0.855	5420	4.2
	-g3	1.14	0.889	6080	4.7
	-g4	1.31	0.922	4590	3.5
	-g5	1.41	0.941	4020	3.1
$\gamma$ -PR	-g1	0.99	0.875	7720	5.9
	-g2	1.24	0.926	4810	3.7
	-g3	1.30	0.946	5240	4.0
	-g4	1.23	0.896	4720	3.6
	-g5	1.30	0.945	3910	3.0

contains the backbone polymers and rings, and was obtained experimentally from the measured weight of swollen gels  $w_{gel}$  and dried gels  $w_{dry}$  as:  $\rho = d_{sol}(w_{dry}/w_{gel})$ , where  $d_{sol}$  is the density of the solvent. Since Eq. 3 is valid only in the rubbery state, the assignment of the two plateaus observed for the polyrotaxane gels is crucial for the estimation of  $M_x$ . The lower plateau modulus at the low frequency limit is about  $10^4$  Pa, which is too low to be the rubbery plateau; the  $M_x$  estimated from the modulus became similar or slightly larger than the molecular weights of the precursor polyrotaxanes, similar to our previously reported polyrotaxane gels<sup>14</sup> (see detailed assignments in ESI†). On the other hand, the higher plateau modulus gives us possible values of  $M_x$  and the average number of CDs between cross-links,  $n_{CD}$ , shown in Table 2 with other experimentally obtained values,  $\rho$  and  $\phi$ . Therefore, the higher plateau can be assigned to the rubbery state, and it is reasonable to employ the higher modulus  $E_\infty$  as  $E_r$  for the estimation of  $M_x$ . Incidentally, after the relaxation, the finite equilibrium modulus is originated from the entropy of uncross-linked CDs that are sliding between cross-links instead of the chain entropy, as suggested by several researches.<sup>33-37</sup>

The estimated  $M_x$  had a clear correlation with the relaxation time  $\tau_s$ . Fig. 7a shows a double logarithmic plot of  $\tau_s$  against the cube of  $M_x$ . In each gel series, the relaxation times  $\tau_s$  are almost proportional to the cube of  $M_x$ , though the relaxation time of the  $\gamma$ -PR gels appears to be longer than that of the  $\alpha$ -PR gels. These cubic power dependences resemble the dependence generally observed in entangled linear polymer melts on the terminal relaxation time. The relaxation time reflects the diffusion dynamics of polymer chains restricted by surrounding chains; the chains can diffuse only along the chain axes, and thus the relaxation time is theoretically proportional to the cube of the molecular weight of the entire chain,  $M$ .<sup>2</sup> However, the only difference is that the relaxation time of polyrotaxane gels depends on  $M_x$ , not  $M$ . Similar restrictions should also be imposed on the chains in polyrotaxane gels, because the chains can diffuse only through the cross-links by sliding. In addition, the chain sliding can lead to the relaxation of the anisotropic orientation of chain segments,<sup>38</sup> which is the origin of rubber elasticity; it is common in both systems that the mechanical relaxations are the result of chain diffusion. Unlike entangled polymer melt that has no limit for diffusion length, polyrotaxane gels cannot flow macroscopically because of the bulky end groups. Thus, the relaxation in polyrotaxane gels can be achieved by the short diffusion distance between cross-links.<sup>15</sup> After the relaxation, CDs can generate the entropic elasticity that is the origin of the stress at the equilibrium state of polyrotaxane gels. Therefore, the characteristic cubic power dependence indicates that the observed mechanical relaxations reflect the dynamics of chains sliding through the cross-links to reach the equilibrium state where the entropy of CDs generates

**Fig. 7** (a) Dependence of the relaxation time  $\tau_s$  on the cube of the average molecular weight of partial chains,  $M_x$ , and (b) on the cube of the normalized molecular weight  $w_{PEG}M_x$ , which is proportional to the contour length of the chain between cross-links,  $L_x$ . Dashed lines depict the slope of the cubic power dependence.

The dynamics of chain sliding, which affect the macroscopic relaxation times  $\tau_s$ , were significantly different for the two ring sizes. To compare the  $\tau_s$  of these two polyrotaxane gels,  $M_x$  must be normalized by the contour length of the chain between cross-links,  $L_x$ , because the  $L_x$  of  $\gamma$ -PR gels is shorter than that of  $\alpha$ -PR gels, even at the same  $M_x$ . As mentioned above,  $\tau_s$  is the time required for diffusion through the length  $L_x$ , which is proportional to the molecular weight of the PEG backbone between cross-links,  $M_{x,PEG}$ , and not to that of the polyrotaxane,  $M_x$ .  $M_{x,PEG}$  can be obtained as a product of  $M_x$  and the weight fraction of PEG,  $w_{PEG}$ :

$$L_x \propto M_{x,PEG} = w_{PEG}M_x. \quad (4)$$

The normalized dependence of  $\tau_s$  is shown in Fig. 7b. This result clearly indicates that the relaxation time of the  $\gamma$ -PR gel is about 5 times longer than that of the  $\alpha$ -PR gel.

The difference in  $\tau_s$  should arise from the difference in friction. The friction likely comes from the cavities of the CDs, because the solvent and backbone are the same in both gels. When the chains slide through the cross-links, the chains are subject to frictional forces from the inner surfaces of the CDs. Such friction should depend on the interactions between the chain and CD in the cavity. It is known that interactions in CD cavities affect the proton spin-lattice relaxation times,  $T_1(^1H)$ .<sup>39</sup>

The  $T_1(^1\text{H})$ s of CDs in  $\alpha$ -PR and  $\gamma$ -PR are summarized in Table 3. The  $T_1$ s were almost independent of ring size, except for that of H5, which is located in the CD cavity near the smaller opening. Because the  $T_1(^1\text{H}5)$ s of the CDs are highly sensitive to the molecules included, this difference arises from the different interactions in the cavities. Although the variation with temperature could determine whether the difference indicated the increase or decrease in interaction, the decrease in temperature broadened the spectra and made the peak separations unable, and the increase in temperature were technically impossible.

The different interactions in PR with different-sized CDs can be explained by the co-inclusion of solvent molecules in the cavities specific to  $\gamma$ -PR, because the loosely threaded  $\gamma$ -CDs have extra cavities that can be filled with solvent molecules. Fig. 8 shows the results of molecular modeling of inclusion complexes of PEG and different-sized CDs in the presence of DMSO solvent molecules. In the  $\alpha$ -PR gel model, the solvent molecules, placed initially in the inclusion cavity, were expelled during the energy minimization process, indicating that no extra space exists. On the other hand, two solvent molecules remained in the cavity of  $\gamma$ -CD with the PEG. A similar co-inclusion of small molecules is known to occur in the extra cavity of a complex between  $\gamma$ -CD and a thin polymer, which stabilizes the loose complex.<sup>40</sup> Such behavior arises from a space-regulating effect, where solvent molecules and substituents of  $\gamma$ -CD can act as regulating moieties for size-mismatched host-guest complexes.<sup>41,42</sup>

**Table 3.** Proton spin-lattice relaxation times,  $T_1(^1\text{H})$  [s], of  $\alpha$ - and  $\gamma$ -PR.

	H1	H2	H3	H4	H5	H6
$\alpha$ -PR	0.90	1.00	0.86	0.87	0.68	0.69 <sup>*1</sup>
$\gamma$ -PR	0.94	1.02	0.90	0.89	0.88	— <sup>*2</sup>

<sup>\*1</sup> The  $T_1$  of H6b overlapped with other resonances. <sup>\*2</sup> This value was not obtained because of the resonance overlap.

The solvents co-included in  $\gamma$ -PR could interact with the inner surface of  $\gamma$ -CD. The cross-sectional view (Fig. 8c) shows that the sulfonyl group of the solvent penetrates the  $\gamma$ -CD cavity. The distance from the oxygen of the sulfonyl group to the C5 of  $\gamma$ -CD is 3.6 Å, which is within the typical distance of CH–O interactions.<sup>43</sup> Such CH–O interactions play a decisive role in the formation of inclusion complexes in solution,<sup>44</sup> though significant shifts in  $^1\text{H}$  NMR peaks are observed only when the rearrangement of interactions occurs slowly due to supporting interactions of neighboring atoms.<sup>45</sup> Notably, another CH–O interaction exists between DMSO and PEG; the distance from the oxygen of DMSO to the nearest carbon of PEG is 3.6 Å. This means that the DMSO bridges PEG and  $\gamma$ -CD. Therefore, the PEG chain is subject to attractive interactions in the  $\gamma$ -CD cavity.

On the other hand, in  $\alpha$ -PR gels, the PEG chain could feel repulsion from the inner surface of  $\alpha$ -CD. Because of the absence of DMSO in the small cavity, the hydrogen atoms of PEG approach the methine protons of  $\alpha$ -CD inside of the cavity, as seen in the cross-sectional view (Fig. 8d). Such contacts between these two non-polar moieties can generate a repulsive force, as many hydrocarbons behave as lubricants exhibiting low viscosity. Therefore, it can be assumed that the

repulsion caused the ideal sliding of the chains through  $\alpha$ -CDs cross-links. Incidentally, possible CH–O interactions between the oxygen of PEG and methine protons of  $\alpha$ -CD seem to be insignificant ( $>3.8$  Å). The co-inclusion of solvent molecules in the extra cavity could significantly change the interaction between the backbone chain and CDs in the cavities, where the attractive interaction mediated by the co-included solvent would decelerate chain sliding. Thus, the change in microscopic molecular dynamics caused the clearly different macroscopic relaxation dynamics of the gels.

**Fig. 8** Molecular models of inclusion complexes of CDs and PEG in the presence of DMSO solvent: (a) top view and (b) side view; only  $\gamma$ -CD allowed the co-inclusion of two solvent molecules. Cross-sectional views of the inclusion cavities of (c)  $\gamma$ -CD and (d)  $\alpha$ -CD. Distances from the oxygen of DMSO to the C5 of  $\gamma$ -CD and nearest carbon of PEG are 3.6 Å.

## Conclusions

We demonstrated that the viscoelastic relaxation dynamics in polyrotaxane gels varies significantly with the size of the ring components. The gels with larger rings showed relaxation times about 5 times slower than those with smaller rings. Both gels with different-sized rings exhibited a common relaxation mechanism: chain sliding along the distance between cross-links. These results indicate that chain sliding through the larger ring cavity was significantly slower. The decelerated chain sliding was attributable to an increase in the interactions between the chain and inner surface of the larger rings, and the interactions may be mediated by solvent molecules interpenetrated in the extra cavity of the larger rings. To the best of our knowledge, this is the first example of a system where the microscopic relative motion, controlled by host-guest interactions, directly affects the mechanical relaxation dynamics. Thus far, many reports have focused on the peculiar statics of polyrotaxane gels caused by chain sliding,<sup>46</sup> without considering interactions between different components. The current study suggests a possible method to control the dynamics of polyrotaxane materials by designing molecular interactions based on host-guest chemistry.

## Acknowledgements

The authors thank Prof. Dr. Hans-Jörg Schneider for fruitful discussions. The authors also thank Prof. Junichi Takeya, Prof. Toshihiro Okamoto, and Dr. Chikahiko Mitsui for help with the NMR measurements. This work was partially supported by Grants-in-Aid for Scientific Research (S) (25220603).

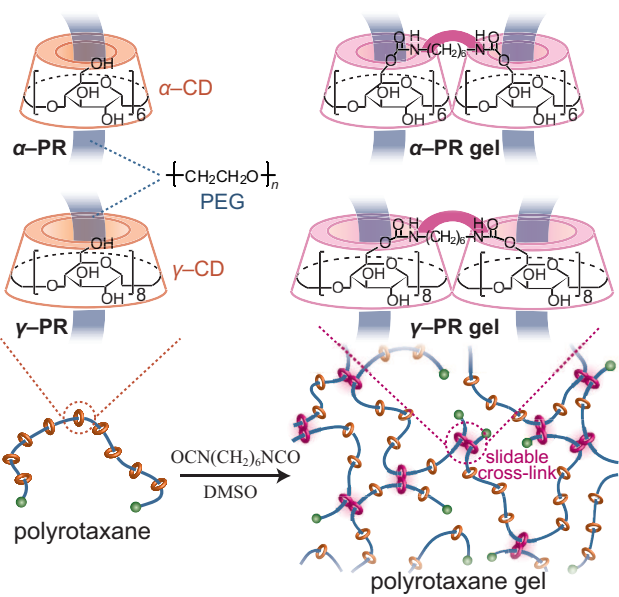
## Notes and references

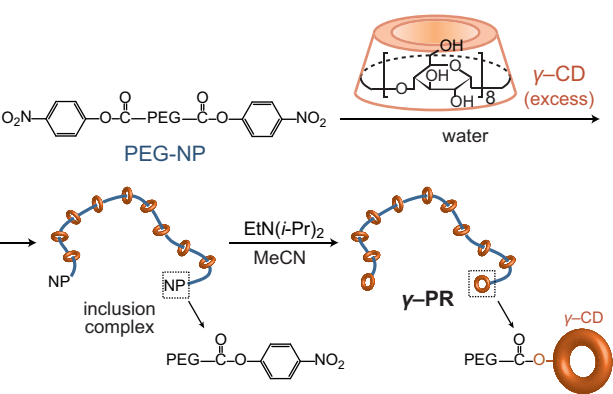
<sup>a</sup> Department of Advanced Materials Science, Graduate School of Frontier Sciences, The University of Tokyo, 5-1-5 Kashiwanoha, Kashiwa, Chiba 277-8561, Japan.

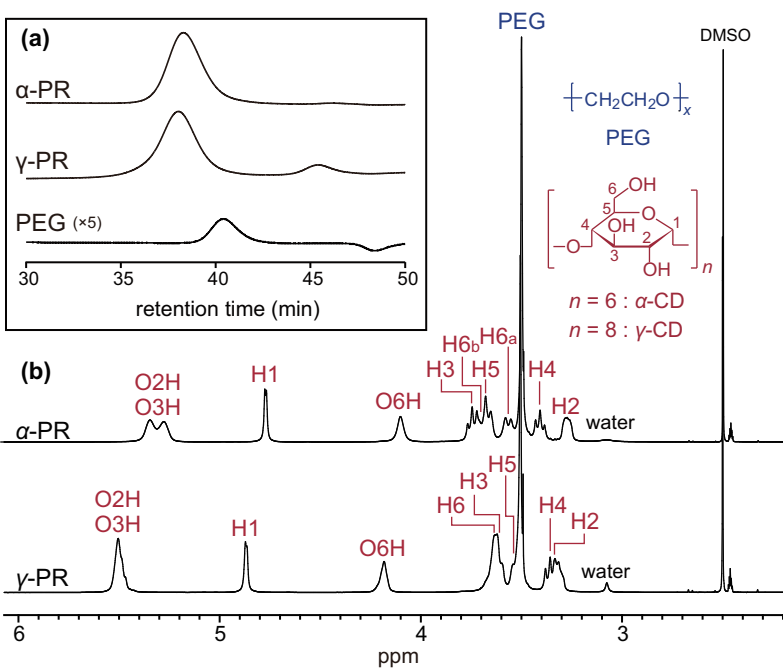
† Electronic Supplementary Information (ESI) available: Syntheses and purification of polyrotaxanes and polyrotaxane gels, calculation of their coverages, detailed assignment of the plateaus observed by viscoelastic measurements, and  $^1\text{H}$ - $^1\text{H}$  COSY NMR spectra. See DOI: 10.1039/b000000x/

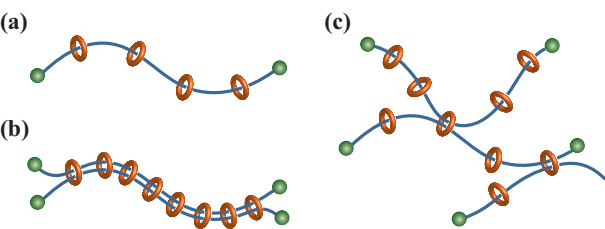
1 T. Kanaya and K. Kaji, *Adv. Polym. Sci.*, 2001, **154**, 88.

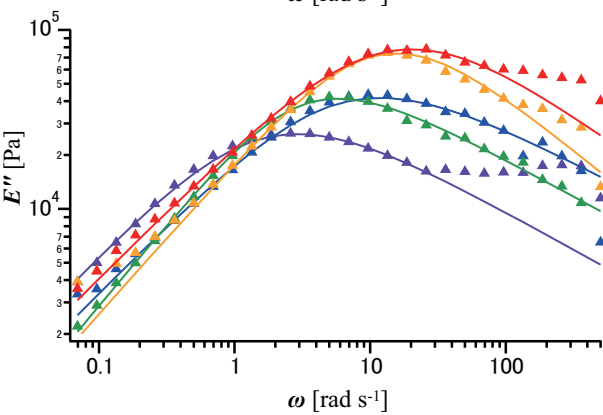
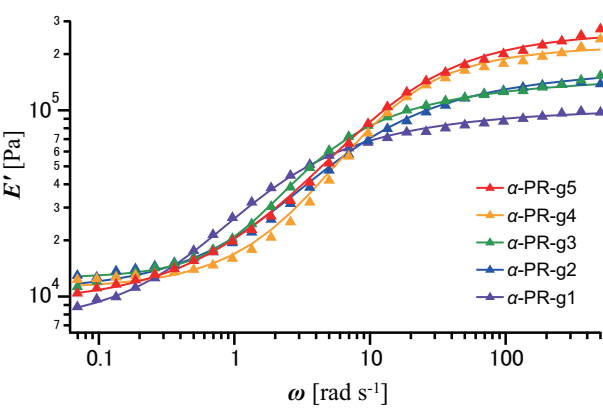
- 2 M. Doi and F. Edwards, *The Theory of Polymer Dynamics*; Oxford Univ. Press: New York, 1986.
- 3 J. A. Brydson, *Relation of Structure to Thermal and Mechanical Properties*, in the chapter "Plastics Materials"; Butterworth-Heinemann; Oxford, 1999.
- 4 H. Watanabe, *Prog. Polym. Sci.*, 1999, **24**, 1253.
- 5 M. Ceccato, P. LoNostro, C. Rossi, C. Bonechi, A. Donati and P. Baglioni, *J. Phys. Chem. B*, 1997, **101**, 5094.
- 6 T. Zhao and H. W. Beckham, *Macromolecules*, 2003, **36**, 9859.
- 7 T. E. Girardeau, J. Leisen and H. W. Beckham, *Macromol. Chem. Phys.* **2005**, *206*, 998–1005.
- 8 K. Mayumi and K. Ito, *Polymer*, 2010, **51**, 959.
- 9 P.-L. Anelli, M. Asakawa, P. R. Ashton, R. A. Bissell, G. Clavier, R. Górski, A. E. Kaifer, S. J. Langford, G. Mattersteig, S. Menzer, D. Philp, A. M. Z. Slawin, N. Spencer, J. F. Stoddart, M. S. Tolley and D. J. Williams, *Chem. Eur. J.*, 1997, **3**, 1113.
- 10 J. W. Choi, A. H. Flood, D. W. Steurman, S. Nygaard, A. B. Braunschweig, N. N. P. Moonen, B. W. Laursen, Y. Luo, E. Delonno, A. J. Peters, J. O. Jeppesen, K. Xu, J. F. Stoddart and J. R. Heath, *Chem. Eur. J.*, 2006, **12**, 261.
- 11 Y. Kawaguchi and A. Harada, *Org. Lett.*, 2000, **2**, 1353.
- 12 G. Wenz, B. Han and A. Müller, *Chem. Rev.*, 2006, **106**, 782, and literature cited therein.
- 13 J. Xue, L. Chen, L. Zhou, Z. Jia, Y. Wang, X. Zhu and D. Yan, *J. Polym. Sci. Part B Polym. Phys.*, 2006, **44**, 2050.
- 14 K. Kato and K. Ito, *Soft Matter*, 2011, **7**, 8737.
- 15 K. Kato, T. Yasuda and K. Ito, *Macromolecules*, 2013, **46**, 310.
- 16 K. Kato and K. Ito, *React. Funct. Polym.*, 2013, **73**, 405.
- 17 S. Havriliak and S. Negami, *Polymer*, 1967, **8**, 161.
- 18 R. Díaz-Calleja, *Macromolecules*, 2000, **33**, 8924.
- 19 A. Harada, J. Li and M. Kamachi, *Nature*, 1992, **356**, 325.
- 20 A. Harada and M. Kamachi, *Macromolecules*, 1990, **23**, 2821.
- 21 Only one report exists thus far using PEG with  $MW = 2000$ : A. Takahashi, R. Katoono and N. Yui, *Macromolecules*, 2009, **42**, 8587.
- 22 A. Harada, *Carbohydr. Polym.*, 1997, **34**, 183.
- 23 A. Harada, J. Li and M. Kamachi, *Nature*, 1994, **370**, 126.
- 24 R. Kawabata, R. Katoono, M. Yamaguchi and N. Yui, *Macromolecules*, 2007, **40**, 1011.
- 25 T. Higashi, F. Hirayama, S. Misumi, H. Arima and K. Uekama, *Biomaterials*, 2008, **29**, 3866.
- 26 K. Kato, H. Komatsu and K. Ito, *Macromolecules*, 2010, **43**, 8799.
- 27 A. Harada, M. Okada and M. Kamachi, *Acta Polymer.*, 1995, **46**, 453.
- 28 J. Li, A. Harada and M. Kamachi, *Polym. J.*, 1994, **26**, 1019.
- 29 Y. Okumura and K. Ito, *Adv. Mater.*, 2001, **13**, 485.
- 30 Y. Okumura, K. Ito and R. Hayakawa, *Polym. Adv. Technol.*, 2000, **11**, 815.
- 31 G. Fleury, C. Brochon, G. Schlatter, G. Bonnet, A. Lapp and G. Hadziioannou, *Soft Matter*, 2005, **1**, 378.
- 32 M. Rubinstein and R. H. Colby, *Polymer Physics*; Oxford University Press: Oxford, UK, 2003.
- 33 K. Ito, *Polym. J.* 2012, **44**, 38.
- 34 K. Mayumi, M. Tezuka, A. Bando and K. Ito, *Soft Matter*, 2012, **8**, 8179.
- 35 M. B. Pinson, E. M. Sevick and D. R. M. Williams, *Macromolecules*, 2013, **46**, 4191.
- 36 A. Bando, K. Mayumi, H. Yokoyama and K. Ito, *React. Funct. Polym.*, 2013, **73**, 904.
- 37 K. Kato, T. Yasuda and K. Ito, *Polymer*, 2014, **55**, 2614.
- 38 T. Karino, Y. Okumura, C. Zhao, T. Kataoka, K. Ito and M. Shibayama, *Macromolecules*, 2005, **38**, 6161.
- 39 M. Okada, M. Kamachi and A. Harada, *J. Phys. Chem. B*, 1999, **103**, 2607.
- 40 W. Herrmann, M. Schneider and G. Wenz, *Angew. Chem. Int. Ed. Engl.*, 1997, **36**, 2511; *Angew. Chem.* 1997, **109**, 2618.
- 41 A. Ueno, K. Takahashi, Y. Hino and T. Osa, *J. Chem. Soc. Chem. Commun.*, 1981, 194.
- 42 A. Ueno, Y. Tomita and T. Osa, *J. Chem. Soc. Chem. Commun.*, 1983, 976.
- 43 G. R. Desiraju, *Acc. Chem. Res.*, 1996, **29**, 441.
- 44 R. E. Gillard, F. M. Raymo and J. F. Stoddart, *Chem. Eur. J.*, 1997, **3**, 1933.
- 45 P. W. Bares, A. M. Beatty, M. Dhanasekaran, B. A. Helfrich, W. Pérez-Segarra and J. Desper, *J. Am. Chem. Soc.*, 2002, **124**, 11315.
- 46 K. Ito, *Curr. Opin. Solid State Mater. Sci.*, 2010, **14**, 28.

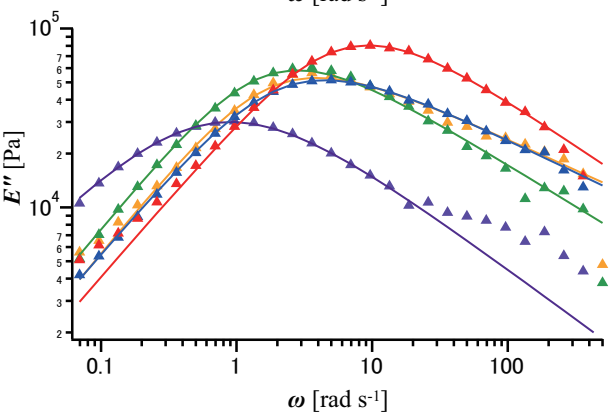
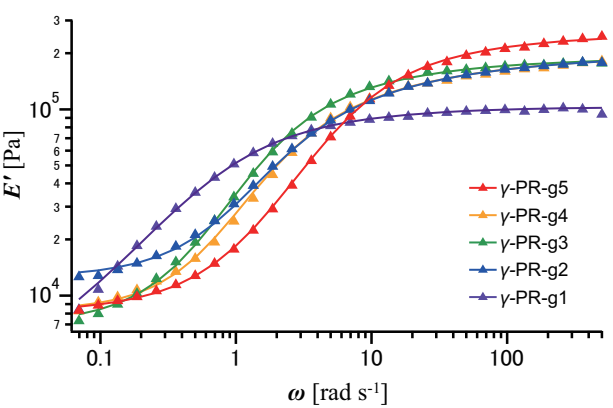


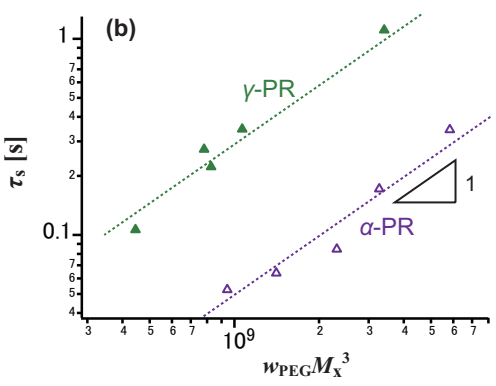
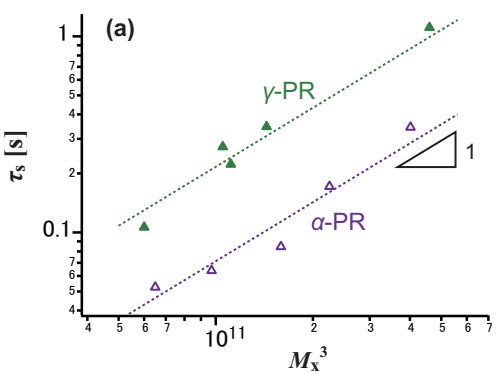


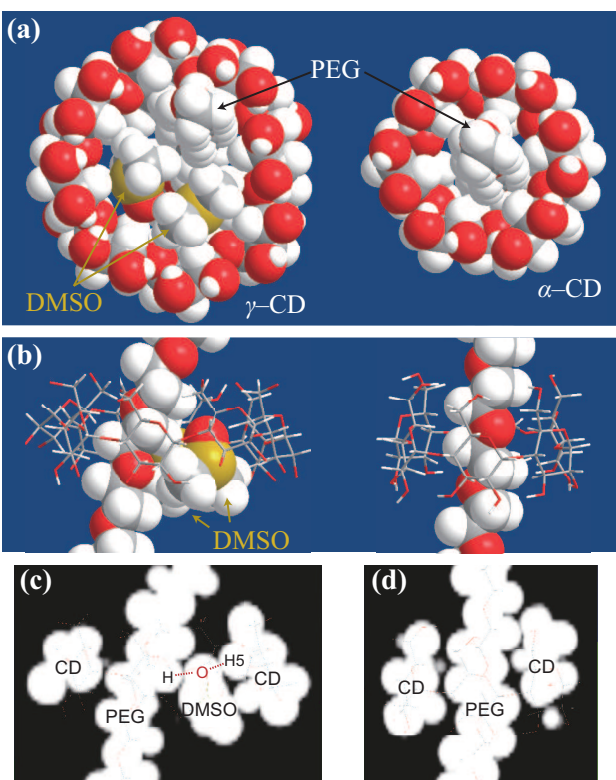












## ARTICLE

## Title Here

Cite this: DOI: 10.1039/x0xx00000x A.N. Authorname,<sup>a</sup> A. N. Authorname<sup>b</sup> and A. N. Authorname<sup>c</sup>,

Abstract text goes here. The abstract should be a single paragraph that summarises the content of the article.

Received 00th January 2012,  
Accepted 00th January 2012

DOI: 10.1039/x0xx00000x

www.rsc.org/

**Table 1.** Summary of polyrotaxanes.

	$M_n$	$M_w/M_n$	coverage <sup>*1</sup>	$w_{\text{PEG}}$ <sup>*2</sup>	yield <sup>*3</sup>
$\alpha$ -PR	64000	1.48	28%	0.24	–
$\gamma$ -PR	87000	1.38	28%	0.20	32%

\*1 Calculated from the molar ratio of the CDs and repeating PEG unit based on a definition described in ESI†. \*2 Weight fraction of PEG in the polyrotaxane. \*3 Yields based on polymers.

**Table 2.** Characteristics of  $\alpha$ - and  $\gamma$ -PR gels.

	$\rho$ [ $10^5$ g/m <sup>3</sup> ]	$\phi$	$M_x$ [g/mol]	$n_{\text{CD}}$
$\alpha$ -PR-g1	0.91	0.838	7380	5.7
-g2	1.12	0.855	5420	4.2
-g3	1.14	0.889	6080	4.7
-g4	1.31	0.922	4590	3.5
-g5	1.41	0.941	4020	3.1
$\gamma$ -PR-g1	0.99	0.875	7720	5.9
-g2	1.24	0.926	4810	3.7
-g3	1.30	0.946	5240	4.0
-g4	1.23	0.896	4720	3.6
-g5	1.30	0.945	3910	3.0

**Table 3.** Proton spin-lattice relaxation times,  $T_1(^1\text{H})$  [s], of  $\alpha$ - and  $\gamma$ -PR.

	H1	H2	H3	H4	H5	H6
$\alpha$ -PR	0.90	1.00	0.86	0.87	0.68	0.69 <sup>*1</sup>
$\gamma$ -PR	0.94	1.02	0.90	0.86	0.88	– <sup>*2</sup>

\*1 The  $T_1$  of H6<sub>b</sub> overlapped with other resonances. \*2 This value was not obtained because of the resonance overlap.